Environmental Science & Technology

pubs.acs.org/est

Article

Abiotic Reduction of Organic and Inorganic Compounds by Fe(II)-Associated Reductants: Comprehensive Data Sets and Machine Learning Modeling

Yidan Gao,[#] Shifa Zhong,[#] Kai Zhang, and Huichun Zhang*

Cite This: https://doi.org/10.1021/acs.est.2c09724

Read Online

ACCESS | Metrics & More | Article Recommendations | Supporting Information

ABSTRACT: Iron-associated reductants play a crucial role in providing electrons for various reductive transformations. However, developing reliable predictive tools for estimating abiotic reduction rate constants (log*k*) in such systems has been impeded by the intricate nature of these systems. Our recent study developed a machine learning (ML) model based on 60 organic compounds toward one soluble Fe(II)-reductant. In this study, we built a comprehensive kinetic data set covering the reactivity of 117 organic and 10 inorganic compounds toward four major types of Fe(II)-associated reductants. Separate ML models were developed for organic and inorganic compounds, and the feature importance analysis demonstrated the significance of resonance structures, reducible functional groups, reductant descriptors, and pH in log*k* prediction. Mechanistic interpretation validated that the models accurately learned the impact of various factors such as aromatic substituents, complexation, bond dissociation energy, reduction potential, LUMO energy, and dominant reductant species. Finally, we found that 38% of the 850,000 compounds in the Distributed Structure-Searchable Toxicity (DSSTox) database contain at least one reducible functional group, and the log*k* of 285,184 compounds could be reasonably predicted using our model. Overall, the study is a significant step toward reliable predictive tools for anticipating abiotic reduction rate constants in iron-associated reductant systems.

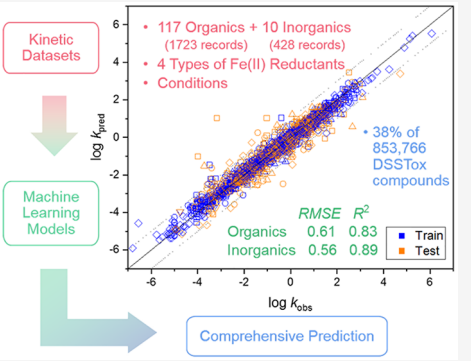

KEYWORDS: *abiotic reduction, Fe(II) reductants, inorganic compounds, machine learning, organic compounds, reactivity prediction*

INTRODUCTION

Reduction is a crucial pathway for the transformation of contaminants in anoxic environments. Ferrous iron, Fe(II), is one of the most important reductants in natural anoxic environments and reduces contaminants containing reducible functional groups. Common reducible functional groups include the nitro group (e.g., explosives, neonicotinoid pesticides), halogens (e.g., chlorinated solvents, fire retardants), −N−O− single bond (e.g., livestock pharmaceuticals), and nitroso group (e.g., disinfection byproducts). Fe(II)-based reductants include aqueous Fe(II), ligand complexed Fe(II) (e.g., Fe(II) complexed with natural organic matter), structural Fe(II) in minerals (e.g., magnetite, FeS, green rust), and sorbed Fe(II) on mineral surfaces (e.g., Fe(II)-goethite).[1] It is important to note that sorbed Fe(II) on iron mineral surfaces is not static and may react with the mineral to become surface- or structure-associated. Different contaminants can be reduced by these Fe(II) reductants through various mechanisms. Environmental conditions such as pH can significantly affect abiotic reduction, as the reduction potentials of the reactants and the dominant reactive species can be greatly influenced by solution pH.[2] However, measuring reduction rates is time-consuming and labor-intensive due to the diversity in reductants, contaminants, and reducing environments. As contaminants may be present in different anoxic environments, such as groundwater, lake sediments, wetlands, and wastewater treatment plants, and some of these contaminants persist, predictive models for the reduction kinetics of all compounds of concern are crucial.

Developing models with broad prediction applicability is a complex task, especially when it comes to predictive models for reduction, as available models are limited in their application and only work for narrowly defined cases. Common models for reduction reactivity, such as quantitative structure−activity relationships (QSARs) and cross-correlations of log*k*, are limited in their applicability, as they only work for specific groups of compounds with the same reducible functional group[3] or two correlated reductants,[4,5] under narrow reaction conditions. Although some QSARs have attempted to incorporate system descriptors like mineral reduction potential,

Special Issue: Data Science for Advancing Environmental Science, Engineering, and Technology

Received: December 26, 2022
Revised: May 3, 2023
Accepted: May 4, 2023

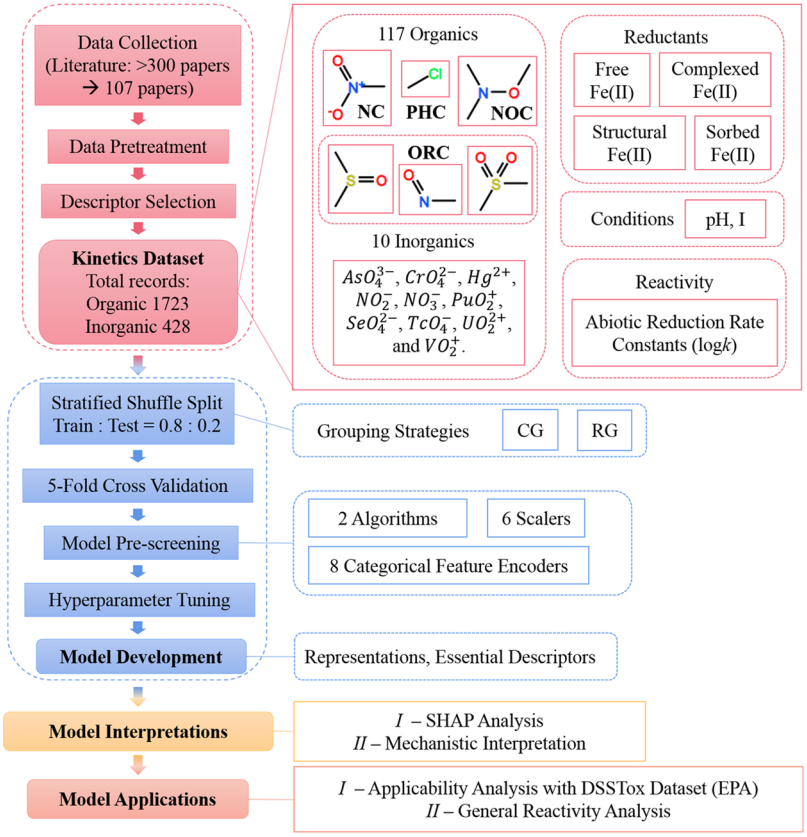

Figure 1. Flowchart of this work. Note: CG = compound grouping; RG = reductant grouping.

mineral physicochemical properties, and pH,[6−8] their ability to account for diverse compounds is still limited. Other modeling approaches, such as molecular modeling and chemoinformatics, mainly predict compound properties rather than handling complex environmental systems.[9] Therefore, it is essential to develop comprehensive models that cover the abiotic reduction of diverse compounds by different reductants under changing conditions.

Moreover, the mechanisms of abiotic reduction for common reducible compounds by different Fe(II)-based reductants are not fully understood,[1] which hinders the development of mechanism-based predictive models. To address this issue, exploring data-driven models for compound reduction reactivity would be timely and necessary, given the recent rapid development and success in ML modeling.[10] Recent studies have successfully developed ML models based on both compound descriptors and system descriptors for the prediction of contaminant reactivity in oxidation,[11] adsorption,[12] and aerobic biodegradation.[13] By leveraging such ML models, it may be possible to develop comprehensive models that can predict the reduction kinetics of diverse compounds by different reductants under varying conditions, without relying solely on mechanistic understanding.

In our recent work,[14] we demonstrated the potential of ML models by developing a single ML model for five groups of reducible compounds, as opposed to five separate QSARs, each QSAR for one group of reducible compounds. However, the kinetic data set we used in our previous research only consisted of 278 log$k$ values for 60 organic compounds tested with one Fe(II) reductant - Fe(II)-tiron complexes. The limited amount of available kinetic data poses a challenge in developing a comprehensive ML model for compound persistence evaluation in various anoxic environments. Furthermore, we face the challenge of a lack of a comprehensive data set that covers the reactivity of all potentially reducible compounds toward all known Fe(II) reductants under different conditions. Unlike compound descriptors, reduction kinetic data are scattered across individual articles and require significant effort to collect. We believe that ML is the best candidate for reactivity prediction, not only because of its ability to handle diverse relationships between inputs and outputs but also because log$k$ can be directly predicted based on measured and calculated descriptors capturing compound, reductant, and condition features without knowing the exact mechanisms.[14] Another advantage of the ML approach is its tolerance to missing values, a common challenge in almost all large data sets,[10] whereas conventional approaches such as QSARs cannot handle this.

This work represents a significant advancement over our previous study due to several key factors. First, the development of models for predicting the reduction kinetics of heterogeneous Fe(II)-based reductants, such as Fe(II)-iron oxides and Fe(II)-containing Fe(III) minerals and clay minerals, has been a major challenge in the literature and has not been achieved before. Second, there is a lack of comprehensive data sets documenting the behavior of complex reduction systems toward a wide range of organic and inorganic compounds. Third, constructing such models is fraught with difficulties, including ensuring data quality, addressing missing data, and selecting appropriate descriptors for training models to achieve reasonable predictions. Finally, even after constructing an ML model, we lack an understanding of its internal processes, such as what it has learned and its applicability to a wide range of reducing systems or

https://doi.org/10.1021/acs.est.2c09724
Environ. Sci. Technol. XXXX, XXX, XXX−XXX

Table 1. Summary of the Abiotic Reduction Kinetic Data Set for Organic Compounds[a]

Model components	Descriptors	Description
Compound	SMILEs	Define compound structures in line notation.
		Converted to MF, Mordred (259), or PaDEL (378) descriptors for modal development.
	Compound concentration	(0.1 μM−264 mM) Define compound initial concentration.
	Acid/base species fractions	Define the fractions of neutral and ionized species based on compound pK_a and solution pH.
	One-electron reduction potential ($E_h^{1\prime}$)	(−0.590 V − −0.287 V) Only for nitroaromatics (405 records).
Reductant	Mineral identity	Categorical feature. Refer to "Reductant_1_Mineral" in the Excel file. Twenty-one types of minerals: structural Fe(II) minerals (magnetite (common, 80 nm, 9 nm), FeS, FeS_2, green rust (X= Cl, CO_3, SO_4, OH, C_{12}), $FeCO_3$, montmorillonite); iron minerals (goethite, hematite, ferrihydrite, lepidocrocite, ferrugious smectite); and noniron minerals (TiO_2, SiO_2, Al_2O_3, kaolin). For homogeneous systems, it is labeled in text "1".
	Surface area	(0−450 m^2/g) A physical-chemical descriptor to characterize mineral phases. "0" for homogeneous systems. 6.1% missing values.
	Mineral loading	(0−100 g/L) Define the concentration of the mineral phase.
	Structural Fe(II) content	(0−1.14 mol/L) Define the Fe(II) concentration in the bulk mineral phase.
	Fe(II)/Fe(III) ratio	(0−1) Refer to it as Fe(II)/total Fe ratio: the fraction of Fe(II) in the total Fe in iron minerals.
	Total Fe content in solid	(0−0.7) Weight ratio of Fe in the mineral phase.
	Sorbed Fe(II) concentration	(0−8.5 mM) Concentration of sorbed Fe(II) on mineral surfaces. 10.7% missing values.
	Standard reduction potential of Fe(II)-iron oxide redox couple (E_H^0)	(0.762 V−1.067 V) Define the reducing ability of sorbed Fe(II). 76.4% missing values.
	Fe(II) concentration	(0−50 mM) Refer to "Reductant_2_Fe(II)" in the Excel file. Define the initial Fe(II) concentration in the aqueous phase.
	Ligand identity	Categorical feature. Refer to "Reductant_3_ligand identity" in the Excel file. Including 69 ligands, such as citrate, cysteine, DMSA, oxalate, thioglycolate, tiron, and Suwannee River humic acid (SRHA). Empty entries are labeled in text "1".
	Ligand concentration	(0−200 mM) Define the ligand concentration.
Condition	pH	pH 1.99−5 (n = 81), 5−9 (n = 1603), 9−12 (n = 39).
	Ionic strength	(0−1 M) Ionic strength was calculated by adding up the contributions of buffers and electrolytes.
Reactivity	log$k$	First-order rate constants, k, ranging from $10^{-5.1}$−$10^{3.1}$ h^{-1}.

[a]The ranges of each descriptor are shown in parentheses. Descriptors were separated into numeric and categorical descriptors (only for reductant descriptors). Categorical descriptors were converted to numerical values via the ML encoder.

https://doi.org/10.1021/acs.est.2c09724
Environ. Sci. Technol. XXXX, XXX, XXX−XXX

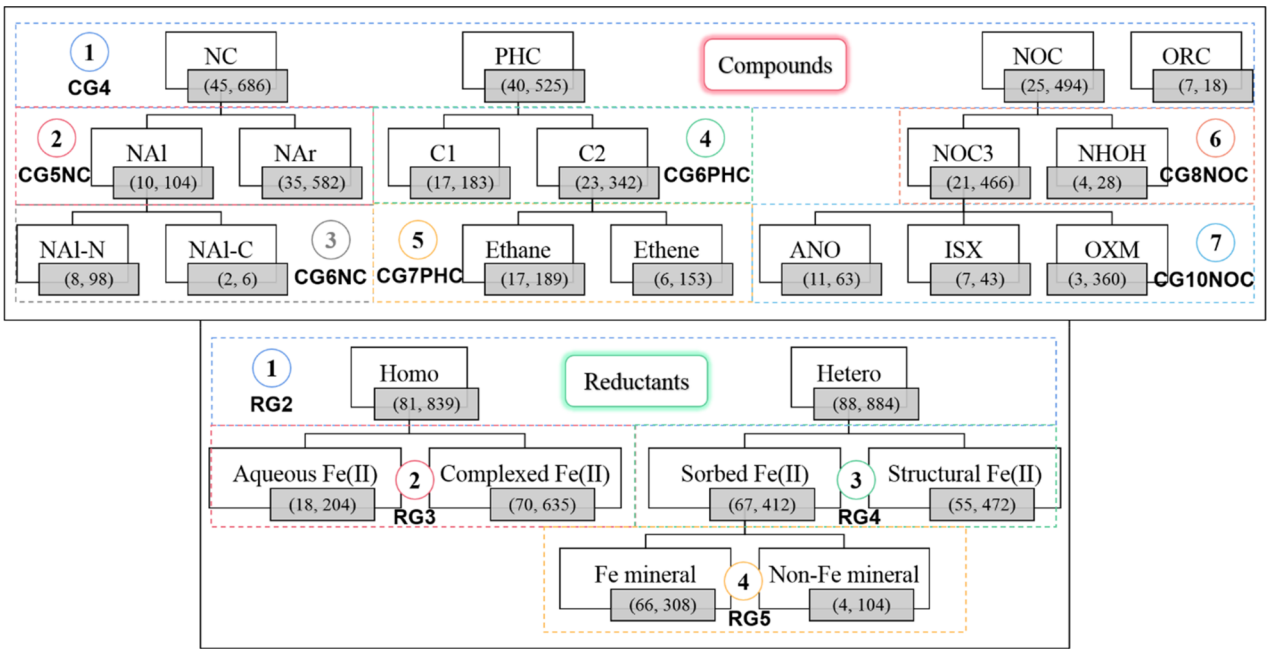

Figure 2. Grouping strategies for organic compounds (top) and reductants (bottom). NCs are divided into nitro-aliphatics (NAls) and nitro-aromatics (NArs). Depending on the α-atom to the -NO_2, NAls were further split into -NO_2 attached to nitrogen (NAl-N) and carbon (NAl-C). PHCs are separated into C_1- and C_2-hydrocarbons. C_1-hydrocarbons contained halogenated methanes, while C_2-hydrocarbons consisted of halogenated ethanes and ethenes. NOCs consist of aromatic N-oxides (ANOs), isoxazoles (ISXs), oximes (OXMs), and hydroxylamines (NHOHs). ORCs include N-heterocyclic nitramine explosive compounds, nitroso compounds (NO), and sulfoxides and sulfones (SOs). The numbers in parentheses in the small gray boxes mean (number of compounds, number of kinetic records) for the compounds or reductants. Boxes with dashed lines indicate further refinement of the groups from top to bottom (e.g., from NCs in group 1 to NArs and NAls in group 2 and then from NAls in group 2 to NAl-N and NAl-C in group 3). In addition to the group numbers (circled numbers inside the dashed boxes), the groups have names, such as CG5NC and RG3, under the group numbers to indicate the sequence of the group refinement (e.g., CG5NC means there are 5 chemical groups with an NC being further refined from CG4). Lines indicate further refinement of the group.

within a broad chemical space. Consequently, this study represents a significant breakthrough in the development of models for predicting reduction kinetics and provides valuable insights into the behavior of complex reduction systems toward various chemicals. The methodology developed in this study addresses the complexity of reduction systems, leading to more accurate predictions and a better understanding of iron-associated reductants in reductive transformations.

The objectives of this study were as follows: 1) to compile a comprehensive data set of abiotic reduction kinetics for all known organic and inorganic compounds using all available Fe(II) reductants; 2) to develop a robust and comprehensive prediction model that estimates compound persistence based on predicted log$k$ values; 3) to create a template/standard for data collection and feature selection to predict abiotic reduction rate constants; 4) to explore methods for interpreting the obtained model and evaluating the extent of model learning in a straightforward manner; and 5) to evaluate the performance and applicability of the model for predicting abiotic reactivity. To achieve these objectives, we conducted a thorough literature review and extracted all relevant kinetic data, reactants, and reaction conditions. We then preprocessed the data by selecting input features and imputing missing data. Different grouping strategies, compound representations, and ML algorithms were compared to obtain the best ML models. The SHAPley Additive exPlanations (SHAP) method[15,16] and comparison with known reduction mechanisms were used to interpret the developed models. Finally, we applied the models to general reactivity analysis for all compounds in the organic data set and identified all potentially reducible compounds in the US EPA Distributed Structure-Searchable Toxicity (DSSTox) Data set.[17] The overall workflow of this work is summarized in Figure 1 (for more details, see Text S1.1 of the Supporting Information (SI)).

MATERIALS AND METHODS

Kinetic Data Sets. All kinetic data used in this study were collected from published journal papers on abiotic Fe(II) reduction. The two kinetic data sets are summarized in an Excel file provided in the SI. The data collection process involved the following steps: (i) searching for relevant keywords in all published research papers between 1995 and 2021 that investigated abiotic Fe(II) reduction; (ii) collecting data from 107 papers out of over 300 collected papers, including descriptors, references, compound names, acid/base dissociation constants (pK_a), dissolved Fe(II) concentration, buffer concentration and pK_a values, temperatures, and rate constants, as summarized in Table 1; (iii) ensuring data quality by checking the experimental design (e.g., control experiments, triplicate experiments), procedure (e.g., rigorous operation in N_2/H_2 atmosphere), and data analysis (e.g., correlation r^2 > 0.90); (iv) preprocessing the data, including converting SMILEs, calculating species acid/base fractions, standard reduction potentials, structural Fe(II) content, and ionic strength, and unifying the data format; (v) selecting initial descriptors based on our understanding of the known mechanisms and the availability of data, as summarized in Table 1 for organic compounds and Table S3 for inorganic compounds; and (vi) converting all the experimentally measured rate constants to first-order constants (k_{obs}, the log

https://doi.org/10.1021/acs.est.2c09724
Environ. Sci. Technol. XXXX, XXX, XXX−XXX

transform is applied later for modeling). See Texts S1.2−S1.5 for more details.

Grouping Strategies. Compounds sharing similar reducible structural features and being reduced in similar reductant systems were manually grouped together, as summarized in Figure 2. *Compound grouping strategies*: The organic data set covered a wide range of organic compounds containing four major reducible functional groups: nitrocompounds (NCs) containing nitro group(s) (-NO_2), polyhalogenated compounds (PHCs) containing halogen atom(s) (-X, X = Cl, Br, F), nitrogen−oxygen containing compounds (NOCs) having −N−O− single bond(s), and other reducible compounds (ORCs) containing additional reducible compounds (only limited numbers of reported logk_{obs}), such as N-heterocyclic nitramine, nitroso compounds, sulfoxides, and sulfones. For compounds containing both -NO_2 and -X, they were grouped based on the reported mechanisms: when the two functional groups were attached to the same aromatic ring, polyhalogenated nitroaromatics were grouped into NArs because -NO_2 was known to be reduced before -X;[18] when -NO_2 and -X were attached to an aliphatic structure, they tended to undergo reductive dehalogenation rather than nitroreduction, so they were grouped into PHCs.[19,20] The inorganic data set contained the top 10 most widely investigated inorganic contaminants, as shown in Figure 1. *Reductant grouping strategies:* This study only involved naturally occurring Fe(II)-associated reductants. Initially, all Fe(II)-reductants were separated into two major groups (RG2): 'Homo' and 'Hetero'. 'Homo' refers to soluble Fe(II)-reductants containing aqueous and complexed Fe(II), while 'Hetero' refers to heterogeneous systems containing structural Fe(II) minerals and sorbed Fe(II) on Fe(III) or non-Fe minerals. Different grouping strategies were applied to refine major compound and reductant groups into subgroups (Text S2.1). Additionally, compound grouping based on calculated similarity levels was conducted for comparison (Text S2.2).

Model Development and Evaluation. We developed ML models to predict log*k* using a five-step procedure: (i) Stratified shuffle split: The data set was stratified based on various grouping strategies to preserve the percentages of records for each group in the training and test data sets. (ii) 5-Fold cross validation: The training data set was split into 5 consecutive folds to minimize model overfitting. One-fold was reserved for model validation, while the remaining 4 folds were used for model training. This process was repeated 5 times, and the average result was used as the final model performance of the training data set. (iii) Model prescreening: The optimal combination of algorithms, encoders, and scalers with the lowest root-mean-square error of the test data set ($RMSE_{test}$) was selected. (iv) Bayesian optimization: The optimal hyperparameters of the selected algorithm, encoder, and scaler were obtained using Bayesian optimization. (v) Development of final models: The final models were developed with the best and simplest representations and essential descriptors selected through Pearson correlation (removing highly correlated numeric features) and Ablative analysis (investigating the importance of each numeric feature by removing one descriptor at a time). For more details, refer to Texts S2.3−S2.7.

Model Interpretation. The developed models were explained using two methods: (i) SHAP analysis, which calculated the feature importance (SHAP values) by comparing the predictive performance of models with and without a certain feature, and (ii) mechanistic interpretation for each group of compounds and the four types of reductants. To explain the reaction mechanisms learned by the organic model without direct input during training, we analyzed the SHAP values and logk_{pred} values. First, we correlated the SHAP values of the Morgan Fingerprint (MF) positions for monosubstituents of nitroaromatics with the reported Hammett constants.[21] Second, we predicted logk_{pred} values for selected compounds under experimental conditions similar to those in studies reporting corresponding mechanisms (as shown in the results). We then built linear correlations between the logk_{pred} values and known descriptors, either extracted from previous studies for PHCs,[22] sorbed Fe(II) reductants,[7] and structural Fe(II) reductants[23] or calculated using environmental software, MINEQL+5.0[24] for complexed Fe(II)[14] and Visual MINTEQ[25] for free Fe(II) and structural Fe(II),[26] under selected conditions. More details can be found in Texts S2.8−2.9.

Model Applicability. Model applicability was determined using two methods: (i) the similarity method by establishing a similarity threshold through computing the average similarity of the test compounds to all training compounds [Compounds with an average similarity score above the established threshold were deemed predictable by the developed model.] and (ii) the functional group method by identifying the MF positions of the reducible functional groups in the organic data set. Compounds containing at least one reducible functional group were deemed potentially predictable for their reduction kinetics, as determined by having 1s in the corresponding MF positions. The applicability of the final organic model was defined as all potentially reducible compounds in the EPA Distributed Structure-Searchable Toxicity (DSSTox) Data Set[17] that had a similarity score above the established threshold. General analysis was conducted by predicting log*k* of organic compounds being reduced in default conditions, which can be used to support exposure assessments (Text S2.10). The default conditions were selected from the most frequently reported reductant systems covering as many different chemical groups as possible in the organic data set (as shown in Results and Discussion). This selection was made to ensure that the predictions were more reliable.

RESULTS AND DISCUSSION

Kinetic Data Sets. The compiled data set contained a total of 2151 abiotic reduction rate constants for 127 compounds. This included 1723 rate constants for 117 organic compounds and 428 rate constants for 10 inorganic compounds, measured under various conditions. The organic data set covered a wide range of compounds (NCs, NOCs, PHCs, and ORCs), reductants (free Fe(II), complexed Fe(II), structural Fe(II), and sorbed Fe(II)), and conditions (acidic, neutral, and basic pH, and varied ionic strength), as shown in Table 1 (organic compounds) and Table S3 (inorganic compounds). The input descriptors included compound descriptors and system descriptors (for reductants and conditions), while the output descriptor was log*k* (Text S3.1). Due to the complexity of the compound structures, reductant types, and reaction conditions in the data sets, it was challenging to identify trends/patterns between logk_{obs} and different descriptors for narrowly defined compound groups and reductant types during the quantitative analysis of the data sets (Text S3.2). Therefore, machine learning models were developed.

https://doi.org/10.1021/acs.est.2c09724
Environ. Sci. Technol. XXXX, XXX, XXX−XXX

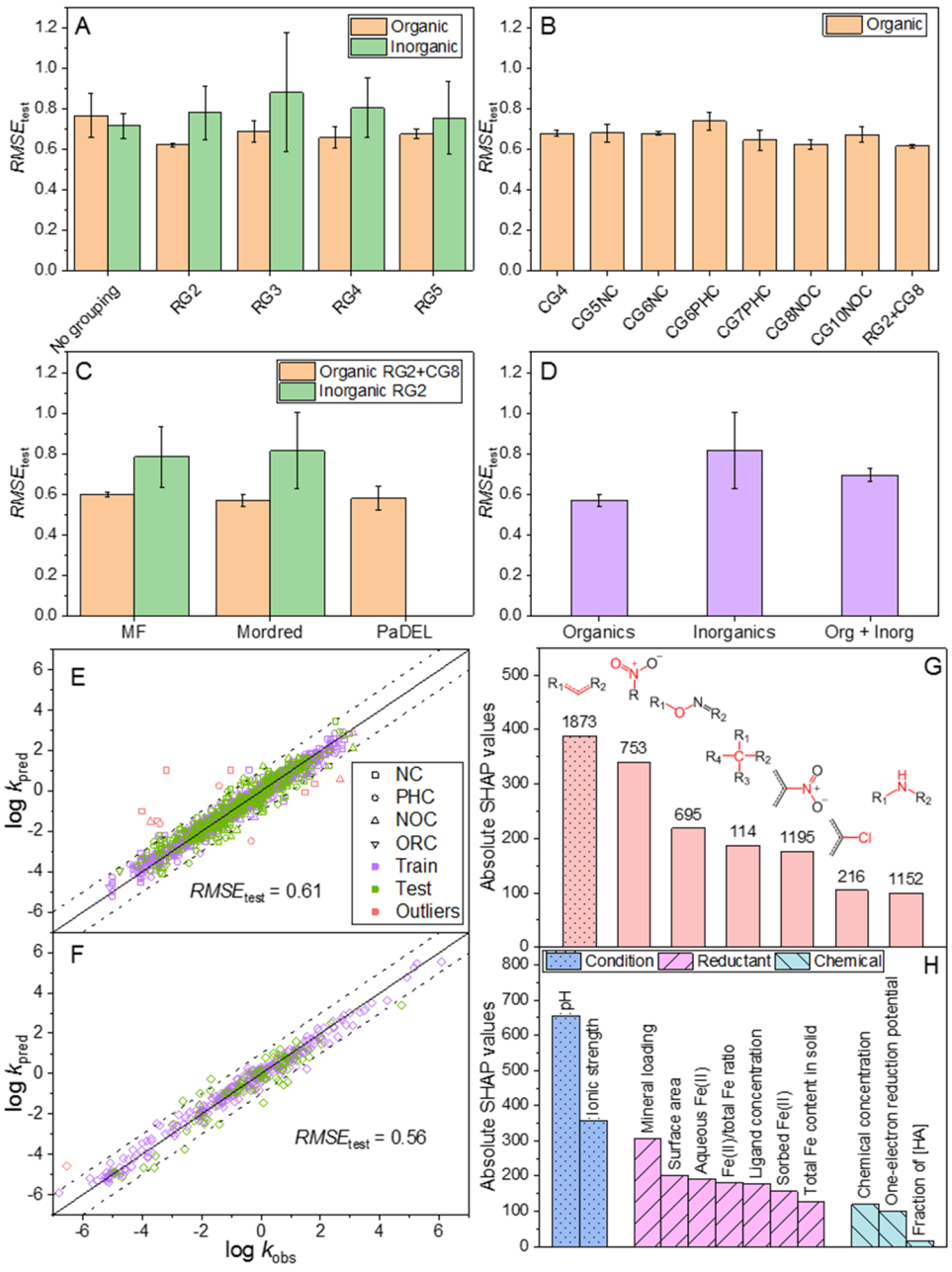

Figure 3. Plots of the model performance ($RMSE_{test}$) with MF based on (A) different reductant grouping strategies, (B) compound grouping strategies, (C) compound representations, and (D) individual models for the organic compounds, inorganic compounds (RG2), and combined Org +Inorg (RG2+CG(8 + 1) data sets, where CG(8 + 1) stands for 8 organic subgroups plus 1 inorganic group). The performance of best models for (E) organic and (F) inorganic compounds. Absolute SHAP values for (G) the most important MF bits of all records in the training data set and (H) the numeric descriptors in the organic data set. Model RG2+CG8 (RS = 90) was employed unless otherwise specified. Error bars are obtained by retraining the models at different random states (RS = 50, 70, 90), which represented different splittings of the records in each group to form different training and test data sets. The outliers in Figure 3E might occur because of (i) the scarcity of kinetic records for a compound toward a specific reductant; (ii) insufficient descriptors to capture reductant characteristics (particle size, dominant reductant species, etc.); and (iii) experimental errors of the original records in the kinetic data set (Table S6).

Model Development. One challenge in developing the model with a relatively small and complex data set was that its performance was not robust when randomly splitting the data into training and test data sets. To ensure that the test set could meaningfully evaluate model performance, different grouping strategies were applied to ensure data similarity between the test and training data sets.[14] The higher the compound similarity between the test and training data sets, the better the predictive performance.[13] $RMSE_{test}$ was selected as the metric to compare model performance in this study (Figure S7). High $RMSE_{test}$ indicates poor model performance, while low $RMSE_{test}$ indicates good model performance. A large $\Delta RMSE$ ($=RMSE_{test} - RMSE_{train}$) indicates overfitting, so a small ΔRMSE is preferred. The model performance with different grouping strategies is shown in Figure 3A,B ($RMSE_{test}$) and Figure S8 ($\Delta RMSE$). The general trends in $RMSE_{test}$ and $\Delta RMSE$ were the same, suggesting that the developed models with better predictive performance

https://doi.org/10.1021/acs.est.2c09724
Environ. Sci. Technol. XXXX, XXX, XXX−XXX

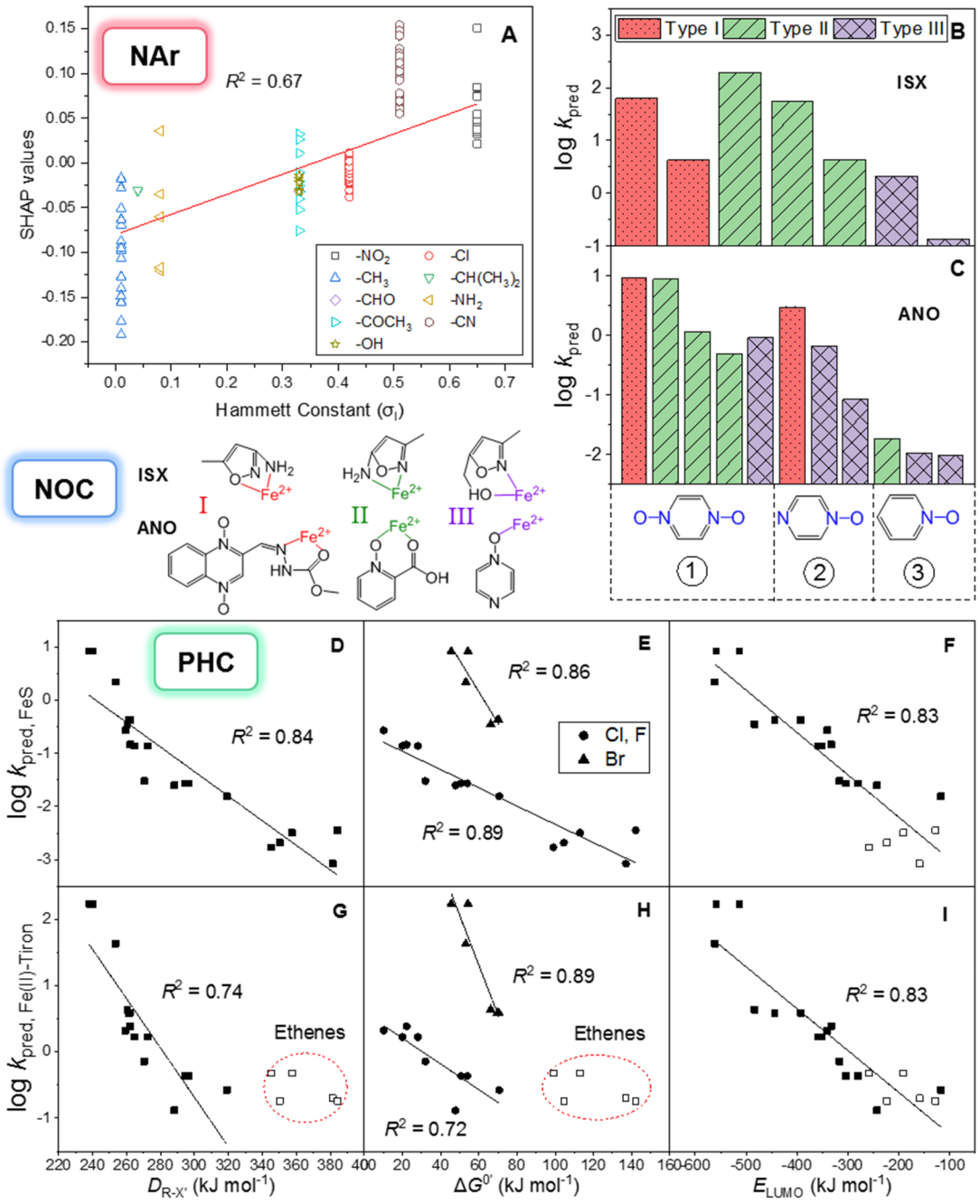

Figure 4. Plots for the mechanistic interpretation of the model (RG2+CG8, RS = 90) observed compound structure effects for (A) nitroaromatics (NArs), (B) ISXs, (C) ANOs, and (D-I) PHCs. (A) Correlations between SHAP values of electron donating/withdrawing groups and Hammett constants (inductive effect). (B−C) logk_{pred} of ISXs and ANOs by Fe(II)-tiron (under the same conditions as in previous studies[28−30]). Red, green, and purple bars indicate type I, II, and III complexations, respectively. Example structures of the three types of complexes for ISXs and ANOs are listed on the left side of Figure 4-C. The numbers in circles represent ANO structures containing ① two −N−O− bonds, ② one −N−O− bond and one ring-N, and ③ only one −N−O− bond. Correlations of logk_{pred} of PHCs by (D-F) FeS and (G-I) Fe(II)-tiron with three compound descriptors: $D_{R-X'}$, $\Delta G^{0'}$, and E_{LUMO}. Solid squares denote the relevant kinetics records were covered in the data set; open squares denote no records in the data set (only model predicted logk_{pred}); circles represent PHC containing Cl- and F-groups; and triangles indicate PHC containing Br-groups. Conditions in (D-F): [FeS] = 33 g/L, Fe(II)/Fe(III) = 1, total Fe content in solid w/w = 0.64, $[Fe(II)]_{ads}$ = 0 mM, I = 0 M, pH = 7, [compound] = 20 μM; conditions in (G-I): [Fe(II)] = 0.5 mM, [tiron] = 10 mM, I = 0.25 M, pH = 7, [compound] = 20 μM.

($RMSE_{test}$) were less likely to have overfitting issues ($\Delta RMSE$). Among all the grouping strategies, RG2+CG8 provided the lowest $RMSE_{test}$ (= 0.62) and $\Delta RMSE$ (= 0.01) and was selected as the organic model, and RG2 had the lowest $RMSE_{test}$ (= 0.78) and $\Delta RMSE$ (= 0.55) and was selected as the inorganic model. The worse performance of the inorganic model might be due to the small data set, which had more than half of the records for Cr(VI) (261 out of 428). The effect of compound grouping strategies on the inorganic compounds was not investigated because the data set only consisted of 10 compounds. Further discussion of the effect of grouping strategies is in Text S4.2. Note that grouping the compounds based on different similarity levels did not improve the model performance and was not investigated further (Figure S9).

https://doi.org/10.1021/acs.est.2c09724
Environ. Sci. Technol. XXXX, XXX, XXX−XXX

Our goal was to develop environmental fate models that accurately represent the essential features of reaction components (i.e., chemicals, reductants, and conditions), instead of relying on different algorithms or improving algorithms based on small data sets. To achieve this, we investigated different compound, ligand, or buffer representations, as shown in Figure 3C and Figure S10. We ultimately chose to represent compounds and ligands using MF and categorical descriptors, respectively, without specifying the buffer identity, as this resulted in the simplest model with the best performance (more details in Text S4.3). Figure 3D indicates that the model performance followed the order of organic compounds > organic+inorganic compounds > inorganic compounds, leading us to develop separate models for organic and inorganic compounds. We provide details on the components used for the final model development in Text S4.3 and Table S5. The final model's performance is shown in Figure 3E,F, with most predictions falling within one log unit of the observed values.

Model Interpretation. Although our ML models have demonstrated exceptional predictive performance, it is essential to ensure that they follow known reaction mechanisms to produce reasonable predictions. To achieve this, we initially quantified the importance of all input features to verify if the models correctly captured the influence of each feature on the compound reactivity. This approach has gained increasing popularity in recent literature for interpreting ML models.[10] However, this technique has limitations as there are numerous reduction mechanisms for various compounds toward different Fe(II) reductants. The feature importance only reflects a feature's contribution to the model prediction and cannot reflect the detailed mechanisms. Therefore, we further interpreted the models by using them to obtain $\log k_{pred}$ of individual compound groups toward selected reductants or of selected compounds toward all four reductant groups. These compound and reductant groups were chosen because they have been extensively examined in the literature regarding their reaction kinetics and mechanisms. QSARs have been established between $\log k_{obs}$ and well-known molecular/reaction descriptors such as reduction potential,[6,7] energy of the lowest unoccupied molecular orbital (E_{LUMO}),[14,22,27] extent of complexation between the compound and reductant,[28−30] and abundance of the dominant reductant species.[18,27,31]

SHAP Analysis. The significance of a descriptor to all compounds was denoted by the sum of the absolute SHAP values of that descriptor for all training records. From left to right in Figure 3G, the ranking of the MF bits illustrates their relative significance in the abiotic rate prediction. Feature 1873, representing a π bond in the form of carbon−carbon double bonds and aromatic rings, had the highest absolute SHAP value so it was the most influential structural moiety for all organic compounds. This demonstrated the significant influence of resonance structures on the compound reactivity. Indeed, feature 1873 was also found to be key for the individual compound groups (Figure S13). The three major reducible functional groups—nitro group (753, 1195), −N−O− single bond (695), and halogen atoms (216: Cl attached to aromatic ring)—were also correctly recognized to be important based on the large absolute SHAP values (Figure 3G). For PHCs, the saturated hydrocarbon structure (114) was shown to be the second most dominant feature, next to the π bond (1873), revealing the importance of aliphatic versus aromatic structures in log*k* prediction for PHCs.[20] Feature 1152 is not a reducible functional group, but NOCs that contain -NH- in the side chain can complex with reactive reductant species to facilitate reduction.[29]

The two condition descriptors were more influential than the reductant descriptors, followed by the chemical descriptors (Figure 3H). Consistent with mechanistic findings that *k* was highly pH dependent,[1] pH was identified as the most important numeric descriptor, because it could affect the dominant species of both the compound and reductant (Text S4.6). The importance of other descriptors was smaller but still non-negligible, as also supported by the ablative analysis results (Figure S12). The species fraction was shown to be the least important because most compounds in the data set were in the neutral forms. The data scarcity, therefore, led to the impact of compound speciation not well-captured by the model. SHAP analysis of the inorganic models and other organic models is discussed in Text S4.6.

Mechanistic Interpretation of the Model Observed Compound Structure Effects. Successful models should capture the mechanistic relationships of log*k*. For NArs, the Hammett constants indicate the electron donating/withdrawing ability of different substituents. Stronger electron withdrawing groups have a larger effect on log*k*, meaning larger SHAP values. As shown in Figure 4A, the SHAP values of the monosubstituents in NArs correlated well with their corresponding Hammett constants. For NOCs, the $\log k_{obs}$ values toward Fe(II)-tiron can be facilitated by the formation of strong complexes and follow the decreasing order of type I > type II > type III.[28−30] Consistently, $\log k_{pred}$ was observed to follow the same order, where type I and II complexations were more reactive than type III complexation for both ISXs and ANOs (Figure 4B,C, Tables S8−S9). Besides, the ring structure of ANOs was proven to have a major influence on $\log k_{obs}$, where the ANOs with two −N−O− bonds were more electron positive, and hence more reactive, than the ANOs with one −N−O− plus one ring-N, followed by the ANOs with one −N−O− alone.[28] This pattern was also learned correctly by the model (Figure 4C).

Studies have reported good linear correlations between $\log k_{obs}$ of PHCs and different compound descriptors (R^2 = 0.80−0.95), such as bond dissociation energy of the weakest R-X bond ($D_{R\text{-}X'}$), the standard free energy of one-electron reduction ($\Delta G^{0'}$), and E_{LUMO}.[22,27] Figure 4D-I demonstrates similar strong linear correlations of $\log k_{pred}$ by two Fe(II) reductants with the three descriptors (R^2 = 0.74−0.89). However, the $\log k_{pred}$ of ethenes by Fe(II)-tiron only showed correlation with E_{LUMO} but not with the other two descriptors (Figure 4G-I). This is because the data set contained kinetic records for the reduction of all PHCs by FeS but only those of methanes and ethanes, not ethenes, by Fe(II)-tiron. The good predictive ability of E_{LUMO} in this work was consistent with the finding in a previous QSAR study[32] where E_{LUMO} was most frequently used regardless of the reaction mechanism. Similar to observations,[27] correlations of $\log k_{pred}$ with $\Delta G^{0'}$ were affected by halogen leaving groups (Cl, F vs Br). Predictions of ethenes are shown as outliers in Figure 4G-H, suggesting that the developed model was unable to expand its knowledge when no records were included. These results revealed that, although we did not specify compound structure effects during the model training process, the model correctly learned their effects in abiotic reduction, validating it to be mechanistically viable. This was likely because these features had been imbedded in the compound structures, which were part of

https://doi.org/10.1021/acs.est.2c09724
Environ. Sci. Technol. XXXX, XXX, XXX−XXX

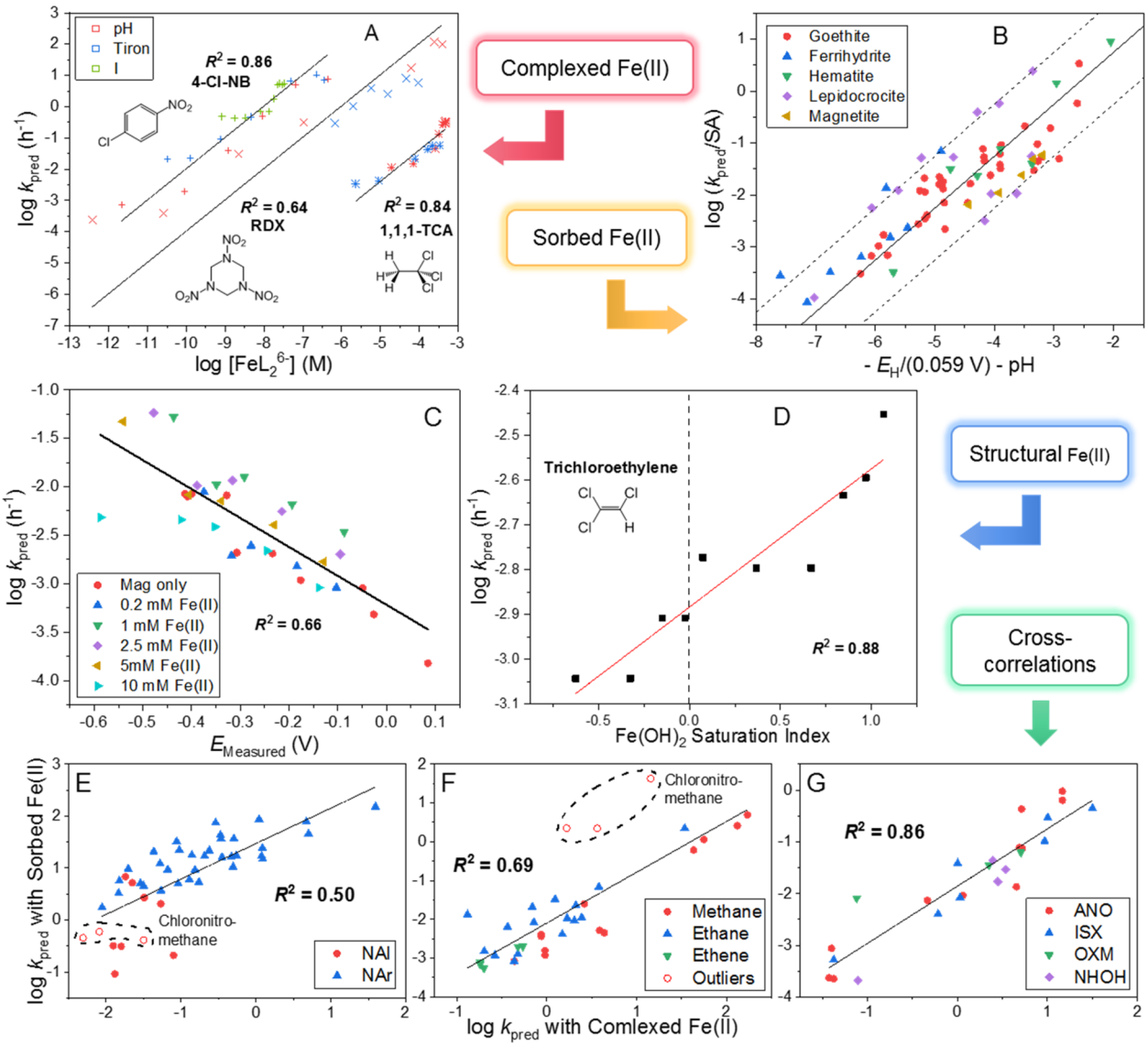

Figure 5. Plots for mechanistic interpretation of the model (RG2+CG8, RS = 90) observed reductant effect based on linear relationships of logk_{pred} with (A) concentration of the 1:2 Fe(II)-tiron complex (FeL_2^{6-}) in Fe(II)-tiron; (B) ($-E_H$/(0.059 V) − pH) of NArs with sorbed Fe(II) (under the same conditions as in reference 7); (C) the measured redox potentials of maghemite-Fe(II) in the presence of different amounts of Fe(II); and (D) concentrations of $Fe(OH)_2^0/Fe(OH)_{2(s)}$ for TCE reduction by magnetite/Fe(II). Cross-correlations for (E) NCs, (F) PHCs, and (G) NOCs between $\log_{red}$ by sorbed Fe(II) (Fe(II)-magnetite for NCs, Fe(II)-goethite for PHCs and NOCs) versus by complexed Fe(II) (Fe(II)-tiron) (under the same conditions as in reference 5). In (A), the concentrations of [FeL_2^{6-}] were calculated by MINEQL+5.0[24] (under the same conditions as in reference 27). In (D), the amount of RMI was quantified as the saturation index (**SatI**) and calculated by Visual MINTEQ[25] based on $\mathbf{SatI} = \log \frac{\mathbf{Q}}{\mathbf{K_{sp}}}$, where **Q** is the ion product of the solid (=[Fe^{2+}][OH^-] for $Fe(OH)_{2(s)}$), and $\mathbf{K_{sp}}$ is the solubility constant of the solid. **SatI** indicates the abundance of $Fe(OH)_2$ in the system. A negative **SatI** value indicates undersaturation, zero indicates solid at equilibrium, and positive **SatI** indicates oversaturation. (Conditions: [Fe(II)] = 5, 10, 15, 20, and 25 mM; I = 0.1 M; and pH = 7.5 and 8.0 in the presence of magnetite.)

the input features. Nevertheless, the obtained model was unable to create new knowledge; instead, they were mainly trained to make predictions based on the given information. See more discussion for the model reflected effects of organic and inorganic compounds in Text S4.7.

Mechanistic Interpretation of the Model Observed Reductant Effects. For complexed Fe(II), logk_{obs} of organic compounds can linearly correlate with the concentration of the dominant reactive species.[18,27,31] Similarly, logk_{pred} of three representative organic compounds, 4- chloronitrobenzene (4-Cl-NB), hexogen (RDX), and 1,1,1-trichloroethane (1,1,1-TCA), toward Fe(II)-tiron correlated well with [FeL_2^{6-}] under changing pH, ionic strength, and tiron concentrations (Figure 5A). Recent work also revealed a good linear correlation between the surface area normalized logk_{obs} of sorbed Fe(II) on different Fe(III) oxides and their reduction potentials (E_H's) under given pH conditions.[7] Similarly, logk_{pred} for the same Fe(III) oxides under the same reported conditions followed a comparable linear correlation (Figure 5B). For structural Fe(II), related mechanistic studies provided evidence for the dominant role of the maghemite-Fe(II) redox couple on the reduction potentials of magnetite suspensions in the presence of aqueous Fe(II);[23] and for $Fe(OH)_{2(s)}$ precipitates being the effective reactive mineral

https://doi.org/10.1021/acs.est.2c09724
Environ. Sci. Technol. XXXX, XXX, XXX−XXX

intermediates (RMIs) in the abiotic reduction of two chlorinated solvents, trichloroethene (TCE) and tetrachloroethene (PCE), by clay minerals in the presence of Fe(II).[33] The obtained $\log k_{pred}$ of TCE and PCE in magnetite/Fe(II) systems linearly correlated with the measured maghemite-Fe(II) redox potential and the abundance of $Fe(OH)_{2(s)}$ (Figure 5C−D for TCE, Figures S16−S17 for PCE). The above three findings strongly confirm that the model captured the reductant effects.

Cross-Correlations. A previous study[5] reported linear correlations of $\log k_{obs}$ of various organic compounds, including substituted nitrobenzenes, polyhalogenated methanes, and NOCs, between two reductant systems: sorbed Fe(II) and complexed Fe(II), that is, cross-correlation (another variation of QSARs). The presence of the cross-correlations can be attributed to the similarity in system descriptors, such as pH, Fe(II) concentration, and reduction potential, that influence the reactivity of these two reductants. However, one challenge was to obtain $\log k$ of different organic compounds under the same conditions because their reactivity might differ a few orders of magnitude and the conditions, such as compound concentration, Fe(II) concentration, ligand concentration, and pH, varied in wide ranges during experimental measurements. With the developed model in this work, we were able to obtain $\log k_{pred}$ for all organic compounds under the same, hypothetical conditions. Compared to the reported cross-correlations with $\log k_{obs}$ (R^2 = 0.76−0.95),[5] this work (Figure S19) showed similar R^2 = 0.84−0.87 for the cross-correlations with the same compounds. Similar R^2 values were also observed for NOCs with a small (0.84 in Figure S19C) versus a large (0.86 in Figure 5G) number of NOCs.

When the cross-correlations were expanded to all NCs, the aromatic and aliphatic structures of the nitro compounds differed in the correlation pattern (Figure 5E), where the aromatic compounds followed a linear cross-correlation, whereas the aliphatic compounds did not. One possible reason is that the applied condition for the model predictions was only relevant for NArs in the training data set, thus causing biased predictions when expanded to NAls. Note that predictions for the NAl reactivity can be improved when more data become available. All PHCs (Figure 5F) examined in this work followed the same cross-correlation, except for three chlorinated nitro-methanes (mono-, di-, trichloronitromethane). When attributing the three chloronitromethanes to NCs (open symbols in Figure 5E), the correlation was consistent with the other NAl compounds. This suggested that the nitro group in these compounds was reduced prior to -Cl based on the model, but this contradicted the experimental results.[19,20] The likely reason for this "error" was that compounds containing multiple reducible functional groups react differently from those only containing one reducible functional group. Sufficient records were also required when training a trustable ML model to capture the dominant reducible functional group(s). The halogenated nitroaromatic compounds had 226 records in the data set, but there were only 16 records for the three chloronitromethanes. So, the model could not identify whether the $-NO_2$ or -X was the primary reducible functional group for halogenated nitro-aliphatic compounds.

Model Applications. The model applicability was first calculated based on similarity levels and showed that query organic compounds with an average similarity above 0.06 toward the training compounds were predictable (Figure S20). Such a low similarity level proved that the developed model was robust and could be applied to a broad range of organic compounds. However, this method did not consider the importance of reducible functional groups in the compound structure, as the similarity level was calculated based on the overall structures. So, we employed the functional group method and determined the model applicability for query compounds based on whether the query compounds had the reducible functional groups. A list of the essential MF bits for each reducible functional group is shown in Table S11. For example, having all 1s at the MF positions of 650, 715, 753, 838, and 1963 suggests the presence of a nitro group.

The DSSTox data set, containing a total of 853,766 environmentally relevant compounds, was our target database to define the applicability domain of the developed model. Among the DSSTox compounds, we found that 5.8% contained $-NO_2$, 6.4% contained -Br, 15.3% contained -Cl, 9.4% contained -F, 0.28% contained ANO, 0.26% contained ISX, 0.20% contained OXM, and 0.01% contained NHOH. Overall, a total of 321,900 compounds (37.7%) in the DSSTox data set contain at least one of the identified reducible functional groups (the other 62.3% are likely not reducible by natural Fe(II) reductants). We then combined the similarity calculation and the functional group method to further evaluate the model applicability of the identified 321,900 compounds and found that 285,184 of them (89%) had the similarity levels above 0.06, so the developed model could provide reasonable estimations for these compounds toward the four types of Fe(II) reductants under different conditions. But because only a small number of organic compounds were in the training data set, future work is warranted to evaluate the uncertainty in the model predictions and to improve the model applicability. Unlike the organic compounds, inorganic compounds have no common reducible functional groups, so the developed model is only recommended for the 10 inorganic compounds included in this work. Finally, the developed models can be used to support exposure assessment by providing $\log k_{pred}$ for a query chemical under conditions of interest (examples of relevant reaction conditions and general analysis of the chemical reactivity under these conditions can be found in Text S4.11).

■ ENVIRONMENTAL IMPLICATIONS

This study developed the largest and most comprehensive data set for abiotic reduction kinetics of all available Fe(II)-associated reductants. Based on this data set, we developed comprehensive models that consider the reductant, compound, and conditions. These models not only predict $\log k$ for compounds in the data set but also provide reasonable reactivity estimations for new query compounds containing reducible functional groups covered in the data set. The predicted reactivity can be used to (i) estimate compound persistence in natural reducing environments and help evaluate its potential risks; (ii) evaluate the potential to use reduction as a natural attenuation or site-remediation approach, based on which one can further engineer the treatment conditions to yield better treatment outcomes; and (iii) gain insights into the reaction mechanisms, such as the rate-limiting steps, by correlating the predicted reduction rate constants ($\log k_{pred}$) with relevant molecular/reaction descriptors.[7]

Despite the aforementioned achievements, further model improvements are still necessary. One limitation of the current models is the lack of sufficient descriptors for solid phases,

https://doi.org/10.1021/acs.est.2c09724
Environ. Sci. Technol. XXXX, XXX, XXX−XXX

such as particle size, extent of aggregation, facets, defects, interlayer cations, conductivity, and other parameters that significantly affect reductant reactivity.[1] For instance, smaller solid particles with higher surface areas are known to be more reactive reductants,[34] but the current models cannot differentiate the reducing ability of the same type of mineral solids with different particle sizes or surface areas due to insufficient data. To enhance our understanding of the reaction mechanisms, we can explore other opportunities such as expanding the range of reducing conditions to cover more records across a wider pH spectrum and increasing the number of records that investigate the impact of various types of dissolved organic matter. By doing so, we can construct a more diverse and comprehensive data set, leading to significant improvements in the performance of our models. Additionally, it is crucial to expand the data set to more complex and realistic reducing environments, such as natural anoxic sediments, where multiple types of minerals and cosolutes coexist and interact, allowing the corresponding model to more accurately predict the reduction reactivity of a given contaminant.

■ ASSOCIATED CONTENT

Supporting Information

The Supporting Information is available free of charge at https://pubs.acs.org/doi/10.1021/acs.est.2c09724.

Text S1. Kinetic data sets, Text S2. Model development, Text S3. Data set analysis, and Text S4. Model development, including figures and tables (PDF)

Incorporates the organic and inorganic data sets, Mordred and PaDEL descriptors, thermodynamic data for iron oxides, model performance, summary of conditions for the general reactivity analysis, Pearson coefficients, ablative analysis, and the MF of the organic compounds (XLSX)

■ AUTHOR INFORMATION

Corresponding Author

Huichun Zhang − *Department of Civil and Environmental Engineering, Case Western Reserve University, Cleveland, Ohio 44106, United States;* orcid.org/0000-0002-5683-5117; Phone: (216) 368-0689; Email: hjz13@case.edu

Authors

Yidan Gao − *Department of Civil and Environmental Engineering, Case Western Reserve University, Cleveland, Ohio 44106, United States*

Shifa Zhong − *Department of Civil and Environmental Engineering, Case Western Reserve University, Cleveland, Ohio 44106, United States;* Present Address: Department of Environmental Science, School of Ecological and Environmental Sciences, East China Normal University, Shanghai 2000241, PR China; orcid.org/0000-0002-5822-0837

Kai Zhang − *Department of Civil and Environmental Engineering, Case Western Reserve University, Cleveland, Ohio 44106, United States;* orcid.org/0000-0003-4058-6512

Complete contact information is available at: https://pubs.acs.org/10.1021/acs.est.2c09724

Author Contributions

#Y.G. and S.Z. contributed equally to this paper.

Notes

The authors declare no competing financial interest.

■ ACKNOWLEDGMENTS

This work was funded by the National Science Foundation Grant CHE-2105005.

■ REFERENCES

(1) Huang, J.; Jones, A.; Waite, T. D.; Chen, Y.; Huang, X.; Rosso, K. M.; Kappler, A.; Mansor, M.; Tratnyek, P. G.; Zhang, H. Fe(II) Redox Chemistry in the Environment. *Chem. Rev.* **2021**, *121* (13), 8161−8233.

(2) Schwarzenbach, R. P.; Gschwend, P. M.; Imboden, D. M. *Environmental Organic Chemistry*, 3rd ed.; John Wiley & Sons P&T: 2017.

(3) Klausen, J.; Troeber, S. P.; Haderlein, S. B.; Schwarzenbach, R. P. Reduction of Substituted Nitrobenzenes by Fe(II) in Aqueous Mineral Suspensions. *Environ. Sci. Technol.* **1995**, *29* (9), 2396−2404.

(4) Pecher, K.; Haderlein, S. B.; Schwarzenbach, R. P. Reduction of Polyhalogenated Methanes by Surface-Bound Fe(II) in Aqueous Suspensions of Iron Oxides. *Environ. Sci. Technol.* **2002**, *36* (8), 1734−1741.

(5) Li, X.; Chen, Y.; Zhang, H. Reduction of Nitrogen-Oxygen Containing Compounds (NOCs) by Surface-Associated Fe(II) and Comparison with Soluble Fe(II) Complexes. *Chemical Engineering Journal* **2019**, *370*, 782−791.

(6) Fan, D.; Bradley, M. J.; Hinkle, A. W.; Johnson, R. L.; Tratnyek, P. G. Chemical Reactivity Probes for Assessing Abiotic Natural Attenuation by Reducing Iron Minerals. *Environ. Sci. Technol.* **2016**, *50* (4), 1868−1876.

(7) Stewart, S. M.; Hofstetter, T. B.; Joshi, P.; Gorski, C. A. Linking Thermodynamics to Pollutant Reduction Kinetics by Fe^{2+} Bound to Iron Oxides. *Environ. Sci. Technol.* **2018**, *52* (10), 5600−5609.

(8) Zhang, H.; Weber, E. J. Identifying Indicators of Reactivity for Chemical Reductants in Sediments. *Environ. Sci. Technol.* **2013**, *47* (13), 6959−6968.

(9) Tratnyek, P. G.; Bylaska, E. J.; Weber, E. J. In Silico Environmental Chemical Science: Properties and Processes from Statistical and Computational Modelling. *Environ. Sci.: Processes Impacts* **2017**, *19* (3), 188−202.

(10) Zhong, S.; Zhang, K.; Bagheri, M.; Burken, J. G.; Gu, A.; Li, B.; Ma, X.; Marrone, B. L.; Ren, Z. J.; Schrier, J.; Shi, W.; Tan, H.; Wang, T.; Wang, X.; Wong, B. M.; Xiao, X.; Yu, X.; Zhu, J.-J.; Zhang, H. Machine Learning: New Ideas and Tools in Environmental Science and Engineering. *Environ. Sci. Technol.* **2021**, No. 55, 12741.

(11) Zhong, S.; Zhang, Y.; Zhang, H. Machine Learning-Assisted QSAR Models on Contaminant Reactivity Toward Four Oxidants: Combining Small Data Sets and Knowledge Transfer. *Environ. Sci. Technol.* **2022**, *56* (1), 681−692.

(12) Zhang, K.; Zhong, S.; Zhang, H. Predicting Aqueous Adsorption of Organic Compounds onto Biochars, Carbon Nanotubes, Granular Activated Carbons, and Resins with Machine Learning. *Environ. Sci. Technol.* **2020**, *54* (11), 7008−7018.

(13) Huang, K.; Zhang, H. Classification and Regression Machine Learning Models for Predicting Aerobic Ready and Inherent Biodegradation of Organic Chemicals in Water. *Environ. Sci. Technol.* **2022**, *56* (17), 12755−12764.

(14) Gao, Y.; Zhong, S.; Torralba-Sanchez, T. L.; Tratnyek, P. G.; Weber, E. J.; Chen, Y.; Zhang, H. Quantitative Structure Activity Relationships (QSARs) and Machine Learning Models for Abiotic Reduction of Organic Compounds by an Aqueous Fe(II) Complex. *Water Res.* **2021**, *192*, 116843.

(15) Zhong, S.; Zhang, K.; Wang, D.; Zhang, H. Shedding Light on "Black Box" Machine Learning Models for Predicting the Reactivity of HO Radicals toward Organic Compounds. *Chemical Engineering Journal* **2021**, *405*, 126627.

(16) Lundberg, S. M.; Lee, S.-I. A Unified Approach to Interpreting Model Predictions. *Advances in Neural Information Processing Systems 30 (NIPS 2017)*; 2017, p 10.
(17) US EPA, O. *Distributed Structure-Searchable Toxicity (DSSTox) Database*. https://www.epa.gov/chemical-research/distributed-structure-searchable-toxicity-dsstox-database (accessed 2022-06-10).
(18) Naka, D.; Kim, D.; Strathmann, T. J. Abiotic Reduction of Nitroaromatic Compounds by Aqueous Iron(II)-Catechol Complexes. *Environ. Sci. Technol.* **2006**, *40* (9), 3006−3012.
(19) Chun, C. L.; Hozalski, R. M.; Arnold, W. A. Degradation of Disinfection Byproducts by Carbonate Green Rust. *Environ. Sci. Technol.* **2007**, *41* (5), 1615−1621.
(20) Cervini-Silva, J. Linear Free-Energy Relationship Analysis of the Fate of Chlorinated 1- and 2-Carbon Compounds by Redox-Manipulted Smectitie Clay Minerals. *Environ. Toxicol. Chem.* **2003**, *22* (10), 2298.
(21) Hansch, C.; Leo, A.; Taft, R. W. A Survey of Hammett Substituent Constants and Resonance and Field Parameters. *Chem. Rev.* **1991**, *91* (2), 165−195.
(22) Perlinger, J. A.; Venkatapathy, R.; Harrison, J. F. Linear Free Energy Relationships for Polyhalogenated Alkane Transformation by Electron-Transfer Mediators in Model Aqueous Systems. *J. Phys. Chem. A* **2000**, *104* (12), 2752−2763.
(23) Robinson, T. C.; Latta, D. E.; Leddy, J.; Scherer, M. M. Redox Potentials of Magnetite Suspensions under Reducing Conditions. *Environ. Sci. Technol.* **2022**, *56* (23), 17454−17461.
(24) Schecher, W.; McAvoy, D. *MINEQL+: A Chemical Equilibrium Modeling System*, Ver. 5.0; 2015. https://mineql.com/ (accessed 2019-12-29).
(25) Gustafsson, J. *Visual MINTEQ*, Ver. 3.1; 2013. https://vminteq.lwr.kth.se/ (accessed 2020-08-13).
(26) Benjamin, M. *Water Chemistry*, 2nd ed.; Waveland Press: 2015.
(27) Bussan, A. L.; Strathmann, T. J. Influence of Organic Ligands on the Reduction of Polyhalogenated Alkanes by Iron(II). *Environ. Sci. Technol.* **2007**, *41* (19), 6740−6747.
(28) Chen, Y.; Zhang, H. Complexation Facilitated Reduction of Aromatic *N* -Oxides by Aqueous Fe ^{II} -Tiron Complex: Reaction Kinetics and Mechanisms. *Environ. Sci. Technol.* **2013**, *47* (19), 11023−11031.
(29) Chen, Y.; Dong, H.; Zhang, H. Experimental and Computational Evidence for the Reduction Mechanisms of Aromatic *N* -Oxides by Aqueous Fe ^{II} -Tiron Complex. *Environ. Sci. Technol.* **2016**, *50* (1), 249−258.
(30) Chen, Y.; Dong, H.; Zhang, H. Reduction of Isoxazoles Including Sulfamethoxazole by Aqueous FeII-Tiron Complex: Impact of Structures. *Chemical Engineering Journal* **2018**, *352*, 501−509.
(31) Kim, D.; Strathmann, T. J. Role of Organically Complexed Iron(II) Species in the Reductive Transformation of RDX in Anoxic Environments. *Environ. Sci. Technol.* **2007**, *41* (4), 1257−1264.
(32) Tratnyek, P. G.; Weber, E. J.; Schwarzenbach, R. P. Quantitative Structure-Activity Relationships for Chemical Reductions of Organic Contaminants. *Environ. Toxicol. Chem.* **2003**, *22* (8), 1733.
(33) Entwistle, J.; Latta, D. E.; Scherer, M. M.; Neumann, A. Abiotic Degradation of Chlorinated Solvents by Clay Minerals and Fe(II): Evidence for Reactive Mineral Intermediates. *Environ. Sci. Technol.* **2019**, *53* (24), 14308−14318.
(34) Hyun, S. P.; Hayes, K. F. Abiotic Reductive Dechlorination of Cis-DCE by Ferrous Monosulfide Mackinawite. *Environ. Sci. Pollut Res.* **2015**, *22* (21), 16463−16474.

https://doi.org/10.1021/acs.est.2c09724
Environ. Sci. Technol. XXXX, XXX, XXX−XXX